Eur. Phys. J. A (2012) **48**: 182
DOI 10.1140/epja/i2012-12182-6

THE EUROPEAN PHYSICAL JOURNAL A

Letter

Measurement of the differential cross-section and deuteron vector analyzing power in dp-elastic scattering at 2.0 GeV

V.V. Glagolev, V.P. Ladygin, N.B. Ladygina, and A.A. Terekhin[a]

Joint Institute for Nuclear Researches, LHEP, Dubna, Russia

Received: 3 July 2012 / Revised: 8 October 2012
Published online: 12 December 2012

Communicated by P. Salabura

Abstract. Measurements of the angular dependence of the vector analyzing powers A_y and differential cross-section in dp-elastic scattering at $T_d = 2\,\text{GeV}$ for the angular range from 10° to 35° in the c.m.s. have been performed. The obtained data are in good agreement with the existing data and theoretical calculations made in the framework of the relativistic multiple scattering model.

1 Introduction

Lately the interest to simple nuclear reactions has increased significantly. The advantage of these processes is that such reactions can be studied in an almost model-independent manner, using a minimum number of free parameters. Interactions between nucleons, electrons and light nuclei provide the information for theoretical description of the nuclear forces. In particular, dp-elastic scattering gives information which is related to the mechanism of nucleon-nucleon interaction and the short-range deuteron structure.

Different approaches are applied to describe dp-elastic scattering at low and intermediate energies: Faddeev calculations in the momentum space [1] and configuration space [2], and variational calculations based on the solution of the three-particle Schrödinger equation [3–5]. The momentum-space Faddeev equations for three-nucleon scattering can now be solved with high accuracy for the most modern two- and three-nucleon forces below 200 MeV/nucleon of the projectile energy [6, 7]. The influence of the Coulomb interaction is appreciable at the energies below 30 MeV, while it considerably reduces at 65 MeV. The discrepancy between theory and experiment is increasing with increasing energy, indicating the possibility of relativistic effects. It should be noted, that this discrepancy is less at small angles than at the larger ones. Most of investigations on the polarization observables nd- and dp-elastic scattering cover the energies below the pion production threshold [8–14]. The experiments were performed to test various models of 2N and account for 3N forces (3NF) (see review [15] and references therein). A series of measurements were performed at KVI at the energies of 54–95 MeV/nucleon for the angular range of $30^\circ < \theta^* < 170^\circ$ in the c.m.s. [13]. Deuteron vector analyzing power data have been obtained at COSY in the domain of very forward polar angles at the energy 65 MeV/nucleon [14]. The precise data were obtained at RIKEN at the energies of 70, 100 and 135 MeV/nucleon [11] for the angular range of $10^\circ < \theta^* < 180^\circ$. The goal of these experiments was to study the 3NF contribution and to test modern models of three-nucleon forces. An analogous experiment was performed in RCNP at the energy of 250 MeV/nucleon [12], where the data on the cross-section and a complete set of proton spin observables were obtained. A complete high-precision set of deuteron analyzing powers for the dp-elastic scattering has been measured at 250 MeV/nucleon [16].The largest discrepancy between the data and theoretical predictions was observed at $\theta^* > 120^\circ$. The results were compared with theoretical calculations using different 2N forces as well as Tucson-Melbourne [17] and Urbana [18] 3N forces. Accounting of the 3NF gives the best agreement with experimental data.

The transition to higher energies will allow one to understand the mechanism of the manifestation of the fundamental degrees of freedom at distances of the order of the nucleon size. The Glauber scattering theory, which takes both single and double interactions, in this case is a classic approach [19, 20]. The experimental data for dp-elastic scattering cover the energy range from 425 to 1500 MeV/nucleon [21–26]. The differential cross-section and vector analyzing power were obtained at 800 MeV for angles $14^\circ < \theta^* < 154^\circ$ in the c.m.s. [22]. The data were obtained at the Brookhaven National Laboratory (BNL) at 1–2 GeV/nucleon for a large momentum [23, 24] and at 1 GeV/n for the angles of $10^\circ < \theta^* < 170^\circ$ [25]. The absolute differential cross-section was measured at 641.3

[a] e-mail: aterekhin@jinr.ru

and 792.7/nucleon MeV in the angular range of 35°–115° and 35°–140°, respectively [26]. Recently, the deuteron vector and tensor analyzing powers were obtained at 440 MeV/nucleon at Nuclotron at JINR [27]. The relativistic impulse approximation [28] does not reproduce experimental data [24], however, the data are well described by the relativistic multiple scattering theory [29].

In this paper we present the experimental data on the angular dependence of the deuteron vector analyzing power A_y and differential cross-section for dp-elastic scattering at 2 GeV obtained at Synchrophasotron at JINR for the angular range of 10°–35° in the c.m.s. The data are compared with the results of the relativistic multiple scattering model [30, 31]. The paper is organized in the following way. In sect. 2 the details of the experiment are given. Section 3 is devoted to the data analysis procedure. The obtained experimental results and their comparison with the theoretical calculations are discussed in sect. 4. The conclusions are drawn in the last section.

2 Experiment

The data have been obtained using the 100 cm hydrogen bubble chamber [32] exposed in the extracted beam at Synchrophasotron (JINR, Dubna). The experimental material consists of two set of data witch were obtained in polarized and unpolarized deuteron beam. The bubble chamber is a proton target and a detector simultaneously. This feature allows to register reaction products in a regime of 4π geometry. The chamber was placed in a strong magnetic field (1.85 T). It provided a reliable identification of secondary particles.

The atomic-beam–polarized ion source "POLARIS" [33] provided the polarized deuteron beam. The nuclear polarization is provided via radio-frequency (RF) hyperfine structure transitions. Two different RF cells of "POLARIS" with the working frequencies of 9.4 MHz and 346.7 MHz have been used to provide the "1–4" and "3–6" transitions, respectively. They have theoretical maximum polarizations of $(p_Z, p_{ZZ}) = (+2/3, 0)$ and $(-2/3, 0)$, respectively. The quantization axis was perpendicular to the beam-circulation plane of the Synchrophasotron. These states have been alternated in the accelerators cycle, and the corresponding mark has been transferred to the apparatus.

The events have been selected on the scanning tables. The mathematical processing has been made by using software packages THRESH [34] and GRIND [35] for the geometrical reconstruction and kinematic identification, respectively. The events have been classified by using information on the particle ionization losses. A chain of support programs has been used to select reactions and record the results to DST (tape of summary results).

Detection efficiency of the dp-elastic events has decreased in the region of small momentum transfers due to a number of methodical features. They are related both to the impossibility to observe the tracks with the momentum less than 80 MeV/c and to the tracks orientation

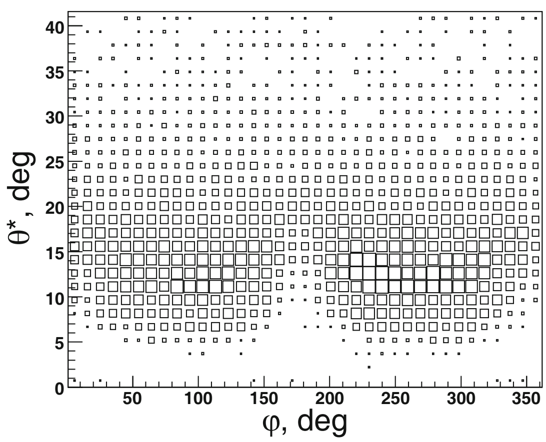

Fig. 1. The correlation of the scattering angle θ^* and the azimuthal angle φ for dp-elastic scattering events.

along the optical axis of the photocamera placed vertically [36]. These effects are demonstrated in fig. 1, where the correlation of the c.m.s. scattering angle θ^* and azimuthal angle φ calculated from the vertical axis is presented.

Systematic losses of the events appear in the dp-elastic scattering channel at small momentum transfers ($|t| < 0.06\,(\mathrm{GeV}/c)^2$). These losses were estimated as 10500 events from the total number of events of the $dp \to X$ interaction 237413, *e.g.*, 4%. The systematic losses for another reactions channels have been found to be negligible. The microbarn equivalent of the events was calculated using the total cross-section for dp- interaction (82.89 ± 0.06 mb) [37] and is equal to $C_o = 0.3342 \pm 0.0007\,\mu$b/event [38]. This value corresponds to the integrated luminosity of the experiment of $\mathcal{L} = 2.992 \pm 0.006\,\mu\mathrm{b}^{-1}$.

3 Data analysis

The dp-elastic scattering differential cross-section has been obtained using the events for the both unpolarized and polarized deuteron beam, while the deuteron vector analyzing power A_y has been evaluated using the events corresponding to the "POLARIS" polarization modes $(-2/3, 0)$ and $(+2/3, 0)$ only [33]. The RF amplitudes for the corresponding hyperfine structure transitions were properly tuned to minimize the asymmetry in the vector polarization values for the both modes, as well as for the tensor polarization admixture, especially, for the mode $(-2/3, 0)$ [39].

The evaluation of the vector polarization of the deuteron beam has been performed using the events from the reaction $dp \longrightarrow ppn$ [40]. The deuteron beam polarization averaged over two polarization modes has been estimated as $p_y = 0.488 \pm 0.061$ by measuring the azimuthal asymmetry of quasi-elastic scattering using the known data on the analyzing powers for the elastic np- and pp-scattering [41, 42] at energy $T_N = 1$ GeV. However, the

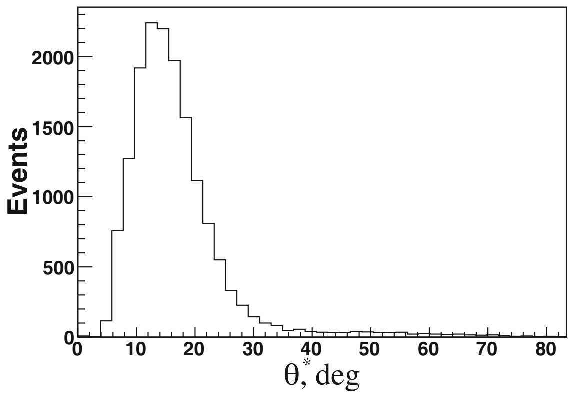

Fig. 2. The *dp*-elastic scattering events as a function of the scattering angle θ^*.

modern partial wave analysis [43] based on the data obtained at Saclay [44–46] and at COSY [47] provides similar values of the analyzing powers for the elastic *np*- and *pp*-scattering. The tensor polarization of the beam was found to be consistent with zero [40].

In general the differential cross-section can be written as [48]

$$\frac{\mathrm{d}\sigma}{\mathrm{d}\Omega}(\theta,\phi) = \frac{\mathrm{d}\sigma_0}{\mathrm{d}\Omega}(\theta)\cdot\left[1+\frac{3}{2}p_Z A_y(\theta)\cos\phi + \frac{1}{2}p_{ZZ}(A_{yy}(\theta)\cos^2\phi + A_{xx}(\theta)\sin^2\phi)\right], \quad (1)$$

where $\mathrm{d}\sigma_0/\mathrm{d}\Omega$ is the unpolarized differential cross-section, p_Z and p_{ZZ} are the vector and tensor deuteron polarizations, respectively, A_y the vector and A_{xx}, A_{yy} the tensor deuteron analyzing powers, θ is the scattering angle, and ϕ is the azimuthal angle with respect to the beam direction.

Since in our case the tensor polarization is equal to zero [40] the differential cross-section can expressed as

$$\frac{\mathrm{d}\sigma}{\mathrm{d}\Omega}(\theta,\phi) = \frac{\mathrm{d}\sigma_0}{\mathrm{d}\Omega}(\theta)\cdot\left[1+\frac{3}{2}p_Z A_y(\theta)\cos\phi\right]. \quad (2)$$

In our case we use the coordinate system related to the optical axis of the photocamera placed vertically [36], therefore, the azimuthal angle $\varphi = \phi + \frac{\pi}{2}$ will be used for further data analysis.

The distribution on the scattering angle θ^* (see fig. 2) has been divided into the consecutive bins. The number of events in each bin has been normalized to the width of the latter. The distribution on the azimuthal angle φ were obtained for each θ^* bin summed over both polarization modes —see examples in fig. 3. One can see that for small scattering angles θ^* the *dp*-elastic scattering events losses have appeared to be symmetrical with respect to the values of the φ-angle of 0° and 180°. The dotted lines in fig. 3 correspond to the boundaries of the regions excluded from the data analysis.

The R value for each chosen interval on θ^* has been calculated as

$$R = \frac{N_\uparrow - N_\downarrow}{N_\uparrow + N_\downarrow}. \quad (3)$$

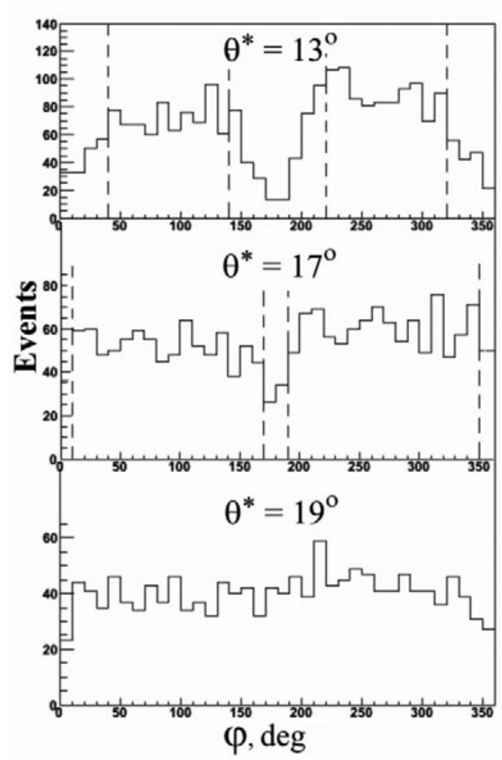

Fig. 3. Dependence of the *dp*-elastic scattering events on the azimuthal angle φ for different values of the scattering angle θ^* summed over both polarization modes. The dotted lines correspond to the boundaries of the regions excluded from the data analysis.

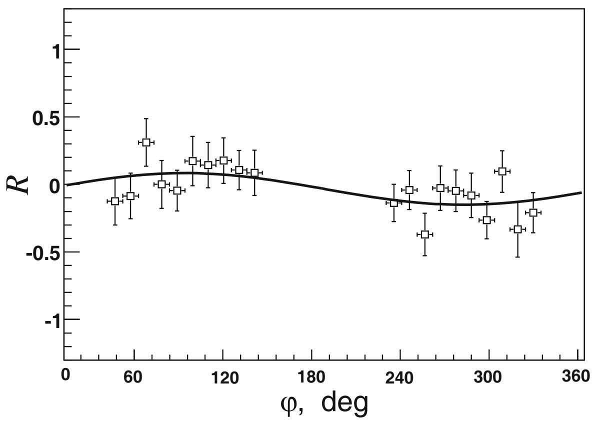

Fig. 4. The R value as a function of azimuthal angle φ for the scattering angle $12^\circ < \theta^* < 14^\circ$. The line is the result of the fit by the function $p_0 + p_1 * \sin(\varphi)$.

Here $N_\uparrow$ and $N_\downarrow$ are φ-dependent numbers of events for the deuteron beam polarized modes $(+2/3, 0)$ and $(-2/3, 0)$, respectively.

An example of the R distribution on the azimuthal angle φ for $12^\circ < \theta^* < 14^\circ$ is shown in fig. 4.

Table 1. Differential cross-section of the *dp*-elastic scattering at 2 GeV.

$\theta_{c.m.s.}$ (deg)	$\mathrm{d}\sigma/\mathrm{d}\Omega$ (mb/sr)	$(\Delta(\mathrm{d}\sigma/\mathrm{d}\Omega))_{stat}$ (mb/sr)	$(\Delta(\mathrm{d}\sigma/\mathrm{d}\Omega))_{sys}$ (mb/sr)
11.0	23.44	0.63	0.31
13.0	19.05	0.47	0.21
15.0	14.14	0.32	0.15
17.0	10.20	0.24	0.10
19.0	6.82	0.17	0.04
21.0	4.44	0.13	0.009
23.0	2.87	0.10	0.006
25.0	1.67	0.07	0.004
27.0	0.99	0.05	0.002
29.0	0.61	0.04	0.001
31.0	0.36	0.03	0.0007
33.0	0.23	0.02	0.0005

Parameters p_0 and p_1 of the function $p_0 + p_1 \cdot \sin(\varphi)$ were determined for each θ^* bin. Here p_0 is the false asymmetry, its value did not exceed 5% for each θ^* bin. The averaged value of p_0 has been found to be -0.025 ± 0.014.

The analyzing power has been obtained from the following expression:

$$A_y = \frac{2}{3}\frac{p_1}{p_y}\,. \tag{4}$$

Here p_y is the vector polarization of the deuteron beam [40]. Since the false asymmetry effect of the A_y value equals $1/(1-p_0^2)$, it was neglected.

The *dp*-elastic scattering differential cross-section has been obtained as follows:

$$\frac{\mathrm{d}\sigma}{\mathrm{d}\Omega}(\theta^*) = \frac{1}{2\pi\mathcal{L}}\frac{N(\cos\theta^*)}{\Delta\cos\theta^*}\,, \tag{5}$$

where $N(\cos\theta^*)$ is the number of events in the bin $\Delta\cos\theta^*$, $\Delta\cos\theta^*$ is the bin width of the $\cos\theta^*$ distribution and $\mathcal{L}$ is the integrated luminosity of the experiment.

4 Results and discussions

The data on the differential cross-section and vector analyzing power A_y are presented in tables 1 and 2, respectively. The following procedure was applied to estimate the systematic error for the cross-section for the θ^* domain with significant event losses. The number of *dp*-elastic scattering events was plotted as a function of the azimuthal angle φ into the histogram with the number of bins equal to 36. Some events were excluded symmetrically with respect to the values of the φ angle of 0° and 180° (see fig. 3). The total number of events in each θ^* bin was calculated as $N_{tot} = N/r$, where $r = n/36$ and N is the remaining number of events in θ^* bin. Here n is the number of the remaining bins. The dependence of the N_{tot} on the r was plotted. The value N_{tot}, in the region where it does not depend on r, was approximated by a constant. The corresponding error was taken as the systematic error

Table 2. Deuteron vector analyzing power A_y of the *dp*-elastic scattering at 2 GeV.

$\theta_{c.m.s.}$ (deg)	A_y	$(\Delta(A_y))_{stat}$
11.0	0.22	0.05
13.0	0.16	0.05
15.0	0.11	0.06
17.0	0.18	0.06
19.0	0.23	0.07
21.0	0.18	0.08
23.0	0.31	0.09
25.0	0.47	0.11
28.0	0.15	0.12
33.0	0.07	0.10

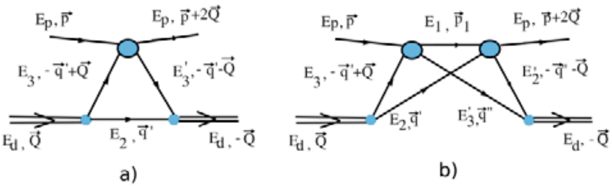

Fig. 5. The diagrams taken into consideration for the calculations within relativistic multiple-scattering model [30,31]: a) single scattering; b) double scattering.

due to the uncertainty in the estimation of the lost events. The total systematic error also includes the uncertainty of the integrated luminosity $\mathcal{L}$. The systematic error for the θ^* domain without losses of the events is defined by the error of the integrated luminosity $\mathcal{L}$ only.

The systematic error for A_y due to accuracy of the beam polarization p_y is estimated to be 13% [40].

The theoretical predictions for the differential cross-section and analyzing power A_y have been obtained in the relativistic multiple-scattering theory frame [30, 31]. In this model the reaction amplitude is defined by the corresponding transition operator. This operator obeys the AGS equation. After iteration these equations up to second-order term over NN t-matrix the reaction amplitude is defined as a sum of the three terms, which correspond to one-nucleon exchange (ONE), single-scattering (SS) and double-scattering (DS) reaction mechanisms. Since the ONE term gives a considerable contribution only at backward angles, this term was not taken into consideration. Thus, the reaction amplitude is defined as the sum of two terms only. Diagrams for SS and DS are presented in fig. 5. All calculations were performed with the CD Bonn deuteron wave function [49]. The parameterization of the NN t-matrix was based on the use of the modern phase shift analysis [43] results.

The differential cross-section as a function of the deuteron scattering angle in the c.m.s. is presented in fig. 6 by the solid symbols. The error bars correspond to the statistical uncertainties only. The open symbols are the data obtained previously [25] with a monochromatic

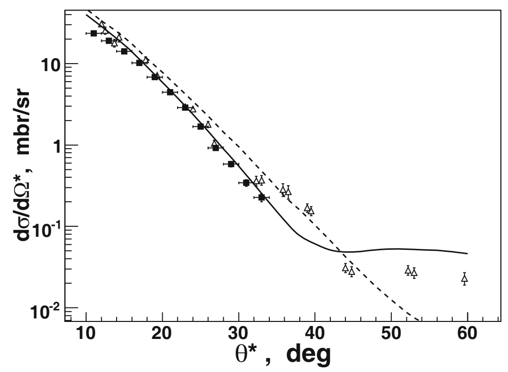

Fig. 6. Solid boxes represent the results of this work. The open triangles are the data from ref. [25]. The dotted and solid lines are the calculations without and with the DS term, respectively.

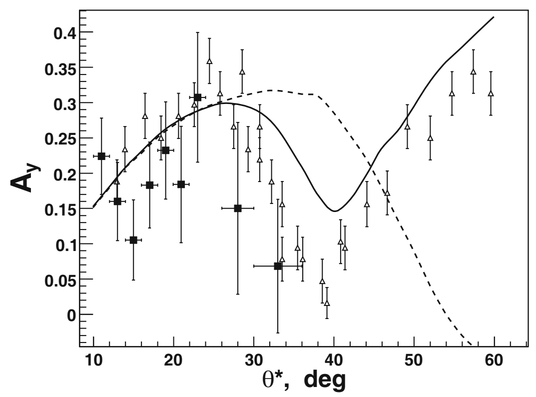

Fig. 7. The solid boxes are the results of this work. Triangles are the data obtained at ANL [43]. The meaning of the lines is the same as in fig. 6.

protons beam at the Brookhaven Cosmotron by using a liquid-deuterium target. A high-resolution spectrometer was used to detect the protons scattered at forward angles. Note that, in the present experiment, the deuteron beam and hydrogen bubble chamber with almost 4π geometry were used. Two sets of data are in agreement within the achieved accuracy in the region where they overlap. The dashed and solid lines are the calculations without and with the DS term, respectively. One can see that the inclusion of the double-scattering term in the calculations, on the one hand, reduces the value of the cross-section in the range of the present measurements and, on the other hand, provides fair agreement with the experimental results up to $\sim 60^\circ$ in the c.m.s.

Our experimental data on the deuteron vector analyzing power A_y are shown in fig. 7 by solid squares. The open triangles are the data obtained at Argonne National Laboratory (ANL) at the Zero-Gradient Synchrotron (ZGS) facility [50]. These data were obtained using a polarized deuteron beam and a 10 cm liquid-hydrogen target. The particles have been registered by a single-arm magnetic spectrometer. In this experiment only the absolute value of the tensor polarization of the beam was measured using the nuclear reaction ${}^3\mathrm{H}(d,n){}^4\mathrm{He}$ at 55 keV. The vector polarization of the beam was not measured, but it was taken as 1/3 from the tensor polarization value. The relative values of the beam vector polarization was monitored during the experiment using the polarimeter based on quasi-elastic *pp*-scattering at thin CH_2 target [50]. Such procedure of the vector beam polarization determination can provide systematic shift of the obtained data on the deuteron vector analyzing power A_y. The statistical uncertainties of both sets of the experimental data are quite large. Therefore, one can conclude that the experimental data are in good agreement, within the achieved accuracy, with each other.

The meaning of the lines is the same as that in fig. 6. One can see that the single-scattering mechanism does not reproduce the experimental data at the scattering angles θ^* larger than 25°. The calculation taking into account the double scattering gives a better agreement with the experimental data in this angular domain. New high-precision deuteron vector analyzing power data are certainly required to make a definitive conclusion on the *dp*-elastic scattering reaction mechanism.

5 Conclusion

The differential cross-section and the deuteron vector analyzing power A_y for the *dp*-elastic scattering have been obtained at $T_d = 2\,\mathrm{GeV}$ for the angular range of 10°–35° in the c.m.s.

The results on the differential cross-section are in agreement, within the accuracy achieved, with the data obtained earlier [25].The data are compared with the calculations performed within the framework of the relativistic multiple-scattering theory [30,31]. It is shown that taking into account the double-scattering term improves the description of the obtained experimental results.

The results on the deuteron vector analyzing power A_y, being in the agreement with the data obtained at ANL [50], are qualitatively described by the relativistic multiple-scattering theory [30,31]. Taking into account the single-scattering term only does not describe the data at $\theta^* > 25^\circ$. The consideration of the double scattering gives a better description of the data at large scattering angles.

The work has been supported in part by RFBF grant *No.* 10-02-00087a.

References

1. H. Witala, Th. Cornelius, W. Glockle, Few-Body Syst. **3**, 123 (1988).
2. J.L. Friar, G.L. Payne, W. Glockle, D. Huber, H. Witala, Phys. Rev. C **51**, 2356 (1995).
3. A. Kievsky, M. Viviani, S. Rosati, Phys. Rev. C **64**, 024002 (2001).
4. M. Viviani, A. Kievsky, S. Rosati, Few-Body Syst. **30**, 39 (2001).
5. A. Deltuva *et al.*, Phys. Rev. C **71**, 064003 (2005).
6. W. Glockle *et al.*, Phys. Rep. **274**, 107 (1996).
7. J. Kuros-Zolnierczuk, H. Witala *et al.*, Phys. Rev. C **66**, 024004 (2002).
8. H. Shimizu *et al.*, Nucl. Phys. A **382**, 242 (1982).
9. H. Amir-Ahmadi *et al.*, Phys. Rev. C **75**, 041001 (2007).
10. E.J. Stephenson *et al.*, Phys. Rev. C **60**, 061001 (1999).
11. K. Sekiguchi *et al.*, Phys. Rev. C **65**, 034003 (2002).
12. K. Hatanaka *et al.*, Phys. Rev. C **66**, 044002 (2002).
13. K. Ermisch *et al.*, Phys. Rev. C **71**, 064004 (2005).
14. I. Ciepal *et al.*, Phys. Rev. C **85**, 017001 (2012).
15. N. Kalantar-Nayestanaki *et al.*, Rep. Prog. Phys. **75**, 016301 (2012).
16. K. Sekiguchi *et al.*, Phys. Rev. C **83**, 061001 (R) (2011).
17. S.A. Coon, H.K. Han, Few-Body Syst. **30**, 131 (2001).
18. B.S. Rudliner *et al.*, Phys. Rev. C **56**, 1720 (1997).
19. V. Franco, R.J. Glauber, Phys. Rev. Lett. **16**, 944 (1966).
20. V. Franco, E. Coleman, Phys. Rev. Lett. **17**, 827 (1966).
21. Y.N. Uzikov *et al.*, JETP Lett. **81**, 303 (2005).
22. E. Winkelmann *et al.*, Phys. Rev. C **21**, 2535 (1980).
23. E. Coleman *et al.*, Phys. Rev. Lett. **16**, 761 (1966).
24. E. Coleman, Technical Report **25**, The University of Michigan (1966).
25. G.W. Bennet *et al.*, Phys. Rev. Lett. **19**, 387 (1967).
26. E. Culmez *et al.*, Phys. Rev. C **5**, 2067 (1991).
27. P. Kurilkin *et al.*, Phys. Lett. B **715**, 61 (2012).
28. R.U. Shepard *et al.*, Phys. Rev. Lett. **50**, 1443 (1983).
29. E. Bleszynski *et al.*, AIP Conf. **150**, 1208 (1986).
30. N.B. Ladygina, Phys. At. Nucl. **71**, 2039 (2008).
31. N.B. Ladygina, Eur. Phys. J. A **42**, 91 (2009).
32. A.V. Belonogov *et al.*, Nucl. Instrum. Methods **20**, 114 (1963).
33. N.G. Anischenko *et al.*, AIP Conf. Proc. **95**, 445 (1983).
34. *CERN T.C.* Program Library, sec. THRESH, 1.3 (1966).
35. *CERN T.C.* Program Library, sec. GRIND, 30.10 (1968).
36. V.V. Glagolev, Preprint JINR, 13-3031 (1966).
37. D.V. Bugg *et al.*, Phys. Rev. Lett. **146**, 980 (1996).
38. V.V. Glagolev *et al.*, Cent. Eur. J. Phys. **6**, 781 (2008).
39. V.G. Ableev *et al.*, Nucl. Instrum. Methods Phys. Res. A **306**, 73 (1991).
40. V.V. Glagolev *et al.*, Z. Phys. A **356**, 183 (1996).
41. M. Marshak *et al.*, Phys. Rev. C **18**, 1 (1978).
42. G.A. Korolev *et al.*, Phys. Lett. B **165**, 4 (1985).
43. `http://gwdac.phys.gwu.edu`.
44. J. Bystricky *et al.*, Nucl. Phys. A **444**, 597 (1985).
45. J. Bystricky *et al.*, Nucl. Phys. B **262**, 715 (1985).
46. J. Ball *et al.*, Nucl. Phys. A **559**, 489 (1993).
47. M. Altmeier *et al.*, Eur. Phys. J. A **23**, 351 (2005).
48. G.G. Ohlsen, Rep. Prog. Phys. **35**, 717 (1972).
49. R. Machleidt, Phys. Rev. C **63**, 024001 (2001).
50. M. Haji-Saied *et al.*, Phys. Rev. C **36**, 2010 (1987).